

A mouse model of autoimmune pancreatitis with salivary gland involvement triggered by innate immunity via persistent exposure to avirulent bacteria

Ikuko Haruta^{1,2}, Naoko Yanagisawa¹, Shunji Kawamura³, Toru Furukawa⁴, Kyoko Shimizu², Hidehito Kato¹, Makio Kobayashi³, Keiko Shiratori² and Junji Yagi¹

The pathogenesis of autoimmune pancreatitis (AIP) remains unknown. Here, we investigated the possible involvement of chronic, persistent exposure to avirulent bacteria in the pathogenesis of AIP. C57BL/6 mice were inoculated with heat-killed *Escherichia coli* weekly for 8 weeks. At 1 week and up to 12 months after the final inoculation, the mice were killed to obtain samples. At 1 week after the final *E. coli* inoculation, marked cellular infiltration with fibrosis was observed in the exocrine pancreas. Cellular infiltration in the exocrine pancreas was still observed up to 12 months after the completion of *E. coli* inoculation. At 10 months after the final inoculation, duct-centric fibrosis became obvious. Inflammation around the ducts in the salivary glands was also observed. Furthermore, sera from heat-killed *E. coli*-inoculated mice possessed anti-carbonic anhydrase, anti-lactoferrin, and antinuclear antibodies. Exposure to *E. coli*-triggered AIP-like pancreatitis in C57BL/6 mice. We propose a hypothetical mechanism for AIP pathogenesis. During the initiation phase, silently infiltrating pathogen-associated molecular patterns (PAMP) and/or antigen(s) such as avirulent bacteria might trigger and upregulate the innate immune system. Subsequently, the persistence of such PAMP attacks or stimulation by molecular mimicry upregulates the host immune response to the target antigen. These slowly progressive steps may lead to the establishment of AIP and associated extrapancreatic lesions. Our model might be useful for clarifying the pathogenesis of AIP.

Laboratory Investigation (2010) **90**, 1757–1769; doi:10.1038/labinvest.2010.153; published online 23 August 2010

KEYWORDS: autoantibody; autoimmune pancreatitis; bacteria; innate immunity; salivary gland involvement

Sarles *et al*¹ first reported a case of pancreatitis with hypergammaglobulinemia that was apparently identical to autoimmune pancreatitis (AIP). In 1992, Toki *et al*² reported four cases with unusual diffuse irregular narrowing of the main pancreatic duct and diffuse enlargement of the entire pancreas with lymphocyte infiltration. In 1995, Yoshida *et al*³ reported 10 cases of chronic pancreatitis caused by autoimmune abnormalities and proposed the concept of AIP.

At present, the features of AIP are recognized as (i) diffuse or segmental narrowing of the main pancreatic duct; (ii) high serum γ -globulin, serum immunoglobulin G (IgG), or IgG4 levels; (iii) marked interlobular fibrosis and prominent infiltrations of lymphocytes and plasma cells; (iv) the presence of autoantibodies; and (v) a unique systemic auto-

immune disease, occasionally associated with extrapancreatic lesions such as sclerosing cholangitis, sclerosing sialadenitis, and retroperitoneal fibrosis.^{4–6} Recently, growing evidence suggests that two clinical and histological patterns of AIP exist (i) lymphoplasmacytic sclerosing pancreatitis (LPSP) or type 1 AIP, which fits the classic description of disease reported from Japan; and (ii) idiopathic duct-centric pancreatitis (IDCP) or type 2 AIP, which is characterized by granulocyte epithelial lesions (GEL) in the pancreas (see Park *et al*⁵ and references therein). IDCP or AIP with GEL is characterized by the massive infiltration of granulocytes in the pancreatic parenchyma and ductal epithelium. Together, AIP with GEL has different clinical characteristics from AIP with LPSP.⁶

¹Department of Microbiology and Immunology, Tokyo Women's Medical University, Shinjuku-ku, Tokyo, Japan; ²Department of Medicine and Gastroenterology, Tokyo Women's Medical University, Shinjuku-ku, Tokyo, Japan; ³Department of Pathology, Tokyo Women's Medical University, Shinjuku-ku, Tokyo, Japan and ⁴Institute for Integrated Medical Sciences, Tokyo Women's Medical University, Shinjuku-ku, Tokyo, Japan
Correspondence: Dr I Haruta, MD, Department of Microbiology and Immunology, Tokyo Women's Medical University, 8-1, Kawada-cho, Shinjuku-ku, Tokyo 162-8666, Japan.
E-mail: haruta@research.twmu.ac.jp

Received 30 April 2010; revised 9 July 2010; accepted 13 July 2010

The pathogenesis of AIP remains unknown.^{4,5} The concept of a syndrome complex or autoimmune exocrinopathy suggests that the pancreas and other organs may possess common target antigens.⁶ A close association with the human leukocyte antigen (HLA) haplotypes DRB1*0405 and DQB1*0401 has been reported in AIP patients.^{7,8} Thus, the antigen presentation of some common peptide to T cells through HLA DRB1*0405 or HLA DQB1*0401 might trigger AIP.⁹ Anti-carbonic anhydrase II (anti-CA-II) and -lactoferrin (anti-LF) are the most frequently detected autoantibodies in human AIP.⁴⁻⁶ Although anti-CA-II and anti-LF are frequently positive in LPSP, they are rarely positive in IDCP.⁵ These autoantibodies might also be involved in the pathogenesis of AIP. Supporting this possibility, Uchida *et al* reported that immunization with CA-II or LF in neonatally thymectomized BALB/c mice led to the apoptosis of duct cells or acinar cells. Furthermore, the adoptive transfer of splenocytes obtained from these immunized mice to nude mice of the same strain induced the same findings.¹⁰ Concerning innate immunity, Muraki *et al*⁸ reported that complement activation through a classical pathway was more likely to be involved in the pathogenesis of AIP. During the early phases of an infection, the complement cascade can be activated on the surface of a pathogen, for example, some bacteria.¹¹

A few reports have shown a Gram-negative bacterial cell wall component, lipopolysaccharide (LPS, endotoxin), to be involved in the pathogenesis of pancreatic inflammatory disease.¹² Laine *et al*¹² reported that the intraperitoneal injection of LPS caused pancreatic acinar cell injury by inducing acinar cell apoptosis or increasing the catalytic activity of pancreatic phospholipase A₂. Vonlaufen *et al* reported that LPS acts as an important triggering factor in the initiation and progression of alcoholic pancreatitis. Repeated challenges of endotoxin in alcohol-fed rats resulted in chronic pancreatic injury, leading to acinar atrophy as well as significant fibrosis.¹³

On the basis of these findings, we speculated that bacterial components and/or molecular mimicry might trigger the onset of autoimmune-mediated chronic pancreatitis. The aim of this study was to investigate whether the chronic persistent exposure of mice to avirulent bacteria might cause immune-mediated pancreatic injury followed by fibrosis, as observed in patients with AIP. Furthermore, we studied antibody production as well as extrapancreatic involvement, events that are frequently associated with human AIP, in mice that were chronically exposed to bacteria.

METHODS

Bacterial Strains and Culture Conditions

A nonpathogenic *Escherichia coli* strain ATCC 25922^T was used for the experiments. Bacteria were cultured in Brain Heart Infusion broth (BD Pharmingen, Franklin Lakes, NJ, USA) aerobically for 18 h at 37°C, with vigorous shaking. The bacteria were harvested and washed twice with phosphate-

buffered saline (PBS; pH 7.4). The bacterial suspensions were then heated at 80°C for 30 min, and then resuspended in PBS. Complete killing was confirmed by 72 h of incubation at 37°C on nutrient agar.

Experimental Mouse Model of Bacteria-Triggered Pancreatitis

C57BL/6 mice were purchased from SLC (Hamamatsu, Japan), whereas RAG2^{-/-} mice^{14,15} were kindly provided by Professor Abe (Research Institute for Biological Sciences, Science University of Tokyo, Japan); all the mice were bred in the animal facility at the Department of Microbiology and Immunology, Tokyo Women's Medical University. Approximately 6-week-old female mice were used for the experiments; all experiments were performed in accordance with the guidelines of the Ethics Review Committee For Animal Experiments, Tokyo Women's Medical University. Mice were injected with 1 × 10⁷ colony forming units of heat-killed *E. coli* in 200 µl of PBS into the peritoneal cavity (i.p.), once a week for a total of 8 weeks. Simultaneously, C57BL/6 mice were inoculated weekly with 200 µl of PBS for 8 weeks and used as controls. Mice were killed under deep anesthesia using diethyl ether at the indicated time after the final inoculation. Tissues were then taken, fixed in 10% formalin, and embedded in paraffin. Simultaneously, sera samples were taken and kept frozen at -80°C until use. Multiple 4-µm-thick sections were used for the pathological examinations.

Pathology

Sections were deparaffinized, stained with hematoxylin and eosin, and evaluated using light microscopy. We graded the histopathological features of the mice pancreas as mild, moderate, or severe based on the severity of periductal cellular infiltrates, periductal fibrosis, and interlobular and acinar involvement: none = 0; mild = 1; moderate = 2; or severe = 3. Each group's pathological score was expressed as the mean ± s.d. To examine the existence of fibrosis, sequential sections were stained with Masson's trichrome stain. Scoring was carried out by two pathologists, SK and TF, who were blinded to the mouse treatment.

To study extrapancreatic involvement in these repeated *E. coli*-inoculated mice, the histopathological features of the salivary glands, liver, and kidney were examined in each mouse.

Immunohistochemistry

Serial sections were subjected to immunohistochemical staining with monoclonal anti-CD3 antibody (clone SP7; Abcam, Tokyo, Japan), B-cell antibody specific for CD45R/B220 (clone RA3-6B2; BD Pharmingen), anti-pan-monocyte/macrophages F4/80 antibody (clone BM8; BMA Biochemicals AG, Augst, Switzerland), polyclonal anti-insulin antibody (DakoCytomation, Kyoto, Japan), and polyclonal anti-glucagon antibody (DakoCytomation). The sections were then

stained using a peroxidase technique with a Vectastain Elite ABC Kit (Vector Laboratories, Burlingame, CA, USA) according to the manufacturer's instructions, followed by staining with hematoxylin.

Serum IgG Levels

Sera obtained from 12 months after the final inoculation with either *E. coli* or PBS were used for the study. Mouse IgG from 5 µl of each serum sample was immunoprecipitated using protein G Sepharose 4 Fast flow (Amersham Biosciences, Uppsala, Sweden) in 1% BSA-PBS. After washing, the bound IgG was run on a 12% acrylamide gel and stained with Coomassie brilliant blue R-250. The intensity of each band on the gel was measured using the ImageJ program/gel analyzer option.¹⁶

Serum Anti-CA-II Antibodies

A measure of 50 µg of CA-II (Sigma Chemicals, St Louis, MO, USA) was boiled in a sample buffer, electrophoresed in a 15% SDS-phase gel, and transferred to a nitrocellulose membrane (Bio-Rad Laboratories, Richmond, CA, USA) using the wet transfer method. The membrane was blocked in TST buffer (10 mM Tris/HCl, 0.9 % NaCl, 0.1 % Tween 20, (pH 7.4)) containing 10% nonfat milk for 20 h at 4°C. Saturated membranes were washed once in TST buffer and were cut into strips. Each strip was incubated with mouse serum diluted at 1/100 in TST buffer containing 2% nonfat milk for 1 h at room temperature. The strips were then washed three times with TST buffer and incubated with horseradish peroxidase (HRP)-conjugated goat anti-mouse IgG antibodies (Biosource, Camarillo, CA, USA). After washing four times, membrane-bound antibodies were detected using 3-amino-9-ethylcarbazole (Sigma Chemicals) containing 0.015% H₂O₂. The intensity of the band obtained from the sera of mice challenged with *E. coli* was compared with that of sera obtained from mice injected with PBS. The density of each band, corresponding to the amount of antibodies bound to the membrane, was measured using the ImageJ program/gel analyzer option.¹⁶

Serum Anti-LF Antibodies

Microtiter plates (MaxiSorp; Nalge NUNC, Roskilde, Denmark) were coated with 10 µg/ml of LF (Sigma Chemicals) in 100 µl of 50-mM sodium carbonate buffer (pH 9.5), and kept overnight at 4°C. The coated wells were washed three times with PBS and blocked with 5% nonfat milk in PBS for 2 h at 37°C. After three washes with PBS, each well was incubated with 100 µl each of mouse serum sample diluted at 1/100 with PBS containing 2% nonfat milk for 1 h at 37°C. The wells were then washed with PBS and incubated with HRP-conjugated goat anti-mouse antibodies (Biosource) for 1 h at 37°C. After three washes with PBS, the bound antibodies were detected with 3,3',5,5'-tetramethylbenzidine (Dako, Glostrup, Denmark). The reaction was stopped by the

addition of 2 M H₂O₂. The plates were read at 450 nm using an ELISA plate reader (Vmax, Molecular Devices, Tokyo, Japan).

Antinuclear Antibody Production in *E. Coli*-Inoculated Mice

Mice sera were used to detect antinuclear antibodies (ANA) using HEp2 (ECACC 86030501) cells.¹⁷ The cells were seeded onto a glass bottom dish (MATSUNAMI, Tokyo, Japan), fixed with 95% ethanol, and blocked with 3% nonfat milk containing 2% TritonX-100 in PBS. The cells were then stained using a 1:100 dilution of each mouse serum sample in PBS, followed by incubation with FITC-conjugated anti-mouse IgG (Jackson ImmunoResearch, Baltimore Pike, PA, USA). The reactions were visualized using a laser-scanning microscope (Carl Zeiss MicroImaging, LSM 510; Carl Zeiss, Jena, Germany).

Statistical Analysis

The densities of the bands were compared using a one-way ANOVA using GraphPad Prism software (San Diego, CA, USA). *P*<0.05 was considered statistically significant.

Spleen Cell Transfer to RAG2^{-/-} Mice

At 1 week after the completion of *E. coli* inoculation, the C57BL/6 mice were killed to obtain their spleen cells. Spleen cells (5×10^7 cells in 200 µl of PBS per mouse) were then intravenously (i.v.) injected into RAG2^{-/-} mice (*n*=6). At 1 week after the spleen cell transfer, the mice were killed to examine the tissues for pathological damage. Simultaneously, spleen cells (5×10^7 cells in 200 µl of PBS per mouse) obtained from C57BL/6 mice inoculated weekly with PBS for 8 weeks were i.v. injected into RAG2^{-/-} mice (*n*=4).

RESULTS

Pathology of *E. Coli*-Inoculated C57BL/6 Mice

We sequentially examined histopathological changes in visceral organs after repeated heat-killed *E. coli* exposure. Throughout this study, we used heat-killed *E. coli*, as in our previous study similar PBC-like autoimmune-mediated cholangitis was observed in the mouse livers of not only live-*Streptococcus intermedius* (*S. i*)-inoculated mice but also heat-killed-*S. i*-inoculated mice.¹⁸ Representative mice at 1 week after the final *E. coli* inoculation showed marked cellular infiltration that consisted of mainly granulocytes, some lymphocytes, and a few plasma cells in the exocrine pancreas. In addition, tubular complexes derived from altered acini, that is, acinar transition, were observed (Figure 1a). The granulocytic infiltration was centered in the ductal systems, and leukocytes were often observed in the lumen with or without the destruction of epithelial cells; these abscesses resembled the granulocytic epithelial lesions that are sometimes observed in patients with AIP (Figure 1a, c, e). Inflammation of the endocrine islets was less pronounced in the *E. coli*-inoculated mice (Figure 1e). Masson's trichrome-positive fibrous stroma was also detected at the

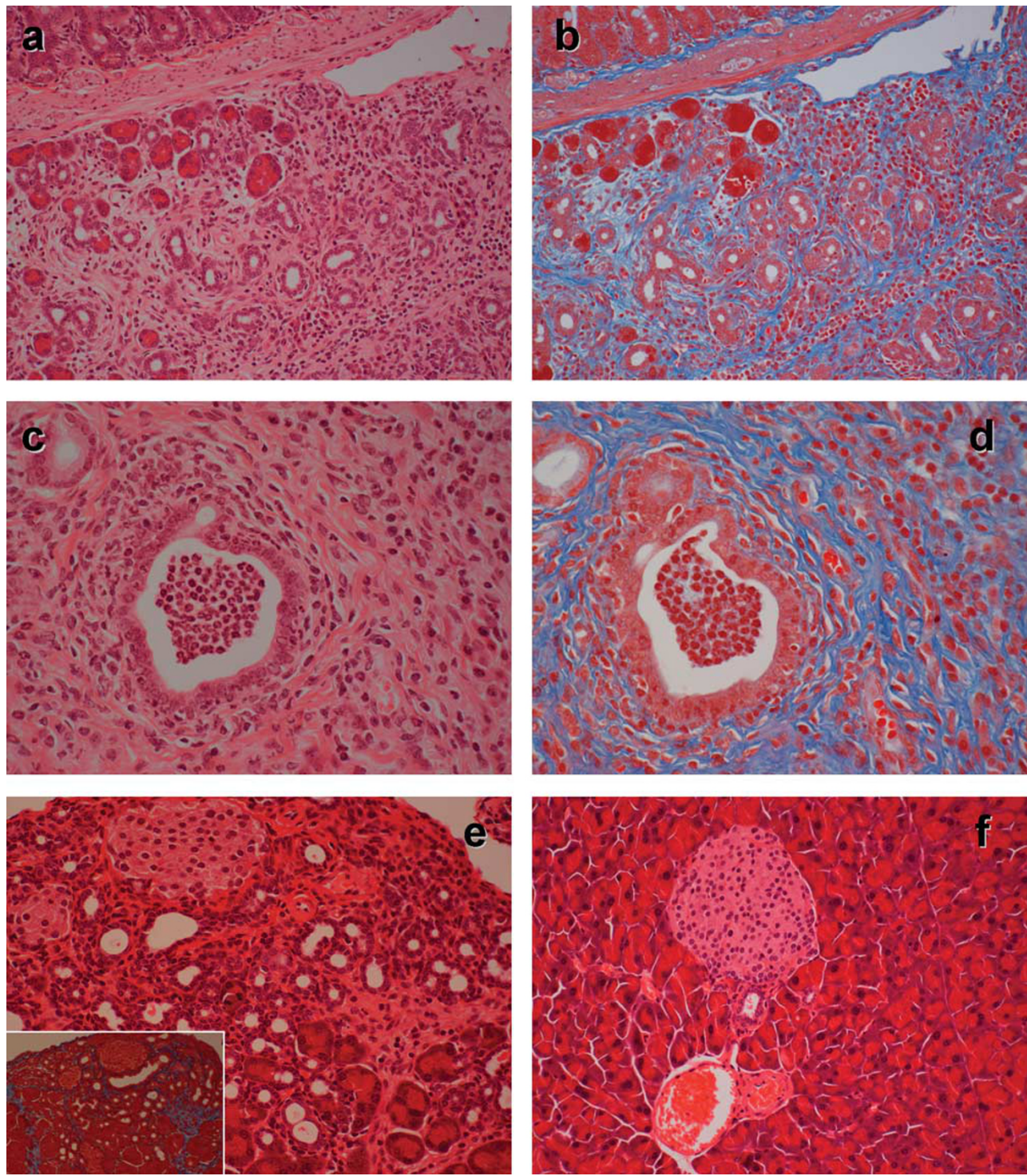
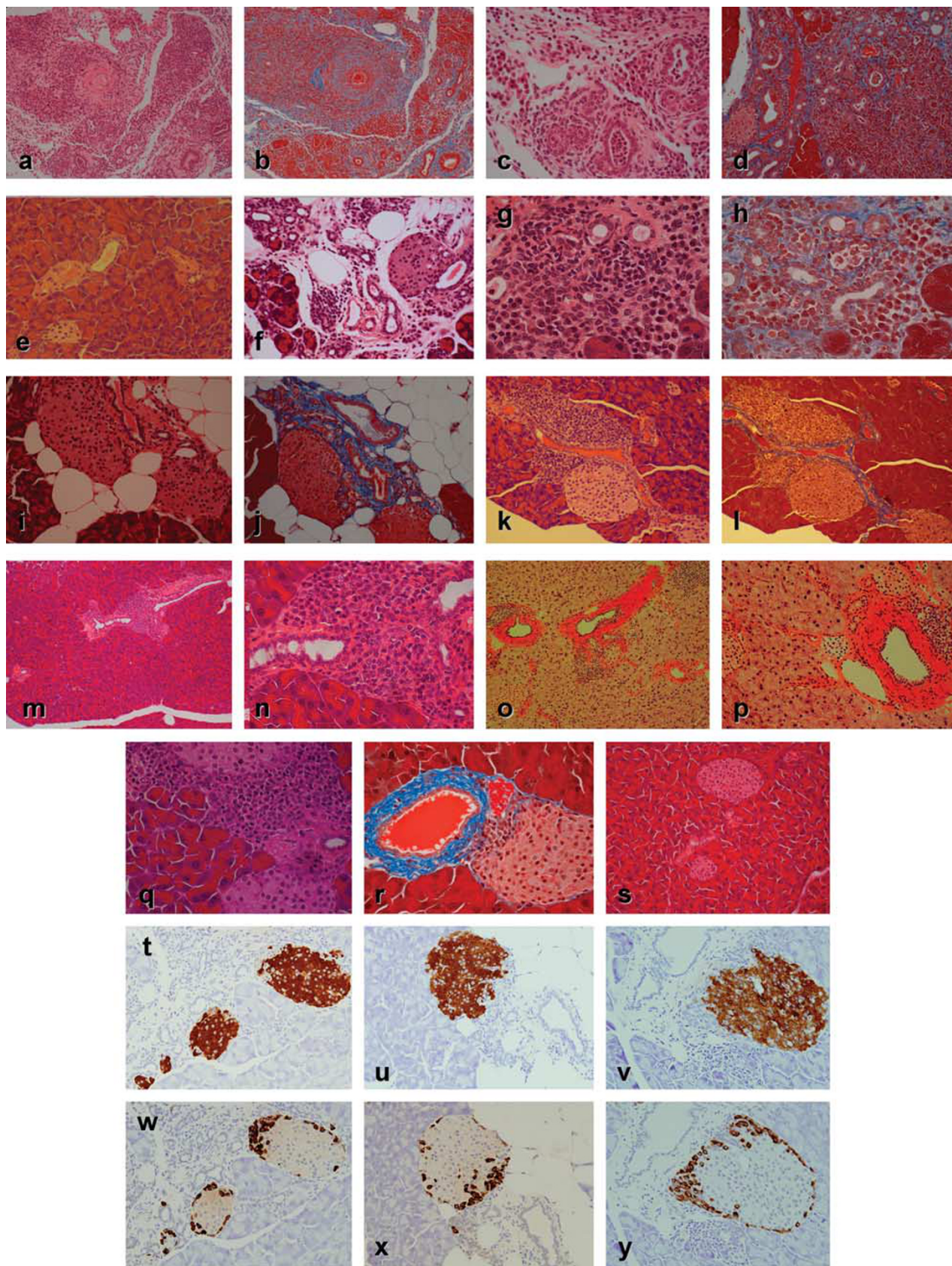


Figure 1 Representative pathological findings of mouse pancreas obtained 1 week after the final *E. coli* inoculation. C57BL/6 mouse pancreas inoculated with heat-killed *E. coli* (**a**, **c**, **e**; H&E staining). Representative Masson's trichrome staining profiles of the pancreas in sequential sections (**b**, **d**, lower left corner of **e**). PBS-inoculated C57BL/6 mouse pancreas (**f**; H&E staining).

Figure 2 Representative pathological findings of mouse pancreas obtained up to 12 months after the final *E. coli* inoculation. Pancreas obtained from a mouse inoculated with heat-killed *E. coli* at 1 month (**a–d**), 2 months (**f–h**), 6 months (**i**, **j**), 10 months (**k–n**), and 12 months (**o–r**) after the final inoculation. C57BL/6 mouse pancreas obtained 1 month (**e**) and 12 months after the final PBS inoculation (**s**). (**a**, **c**, **e–g**, **i**, **k**, **m–q**; H and E staining; **b**, **d**, **h**, **j**, **l**, **r**; Masson's trichrome staining). Immunostaining of insulin (**t–v**) and glucagon (**w–y**) in *E. coli*-inoculated mice pancreas at 2 months (**t**, **w**), 6 months (**u**, **x**), and 12 months (**v**, **y**) after the final *E. coli* inoculation.



site of inflammation around periacinar lesions of the pancreas (Figure 1b, d, e). In the PBS-inoculated mice, no visible changes in periductal cellular infiltrates, periductal fibrosis, or interlobular involvement, the disappearance of acini, and their transition into ductular structures were observed in the pancreas (Figure 1f). Thus, pathological alteration in early stage, that is, at 1 week after the final *E. coli* inoculation, indicated that repeated heat-killed *E. coli* inoculations induced the granulocyte-predominant inflammation and fibrosis in the exocrine pancreas.

After the completion of *E. coli* inoculation, we next investigated long-term pathological alterations. At 1–2 months after the final *E. coli* inoculation, marked cellular infiltrates consisting of lymphocytes, plasmacytes, and granulocytes, associated with ducts (resembling granulocytic epithelial lesions in AIP) were still visible (Figure 2a, c, f, g). Furthermore, Masson's trichrome-positive fibrous stroma was detected at the site of inflammation in periacinar lesions of the pancreas (Figure 2b, d, h). At 1 month after the final PBS inoculation, no visible changes in periductal cellular infiltrates, periductal fibrosis, or acinar transition into ductular structures were observed in the pancreas (Figure 2e). At 6 months after the final *E. coli* inoculation, inflammation in the exocrine pancreas appeared to regress, with some replacement by fatty tissues (Figure 2i, j). At 10–12 months after the final *E. coli* inoculation, without any additional *E. coli* inoculation, inflammatory cellular infiltrates consisting of lymphocytes, plasma cells, and granulocytes, were observed in a more restricted area around the pancreatic ducts in the exocrine pancreas (Figure 2k, l, m, n, o, p). In some areas, segmental inflammation around the peripancreatic duct was observed (Figure 2k, l). Furthermore, Masson's trichrome-positive duct-centric fibrosis was observed in the pancreas (Figure 2l, r). On the other hand, the inflammation of the endocrine islets was much less pronounced (Figure 2d, f, i, k, q), that is, almost no evidence of insulitis was observed in the *E. coli*-inoculated mice (Figure 2t, u, v, w, x, y).

The above findings were not observed in control mice treated with repeated PBS inoculation (Figure 2e, s). The pathological scores are summarized in Figure 3. The predominance of granulocyte infiltration at 1 week after the final *E. coli* inoculation shifted to a predominance of lymphocytes and plasma cells at 2 months after the final *E. coli* inoculation. At long time periods after final *E. coli* inoculation, the infiltrated cell profile was closer to the pathological alterations resembling LPSP in AIP.

Salivary Gland Involvement

We next examined extrapancreatic lesions, long time after the final *E. coli* inoculation in mice. At 6–12 months after the final *E. coli* inoculation, without any additional bacterial inoculation, marked mixed cellular infiltrates consisting of lymphocytes and granulocytes were observed around the ducts in the salivary glands (Figure 4a, b). On the other hand,

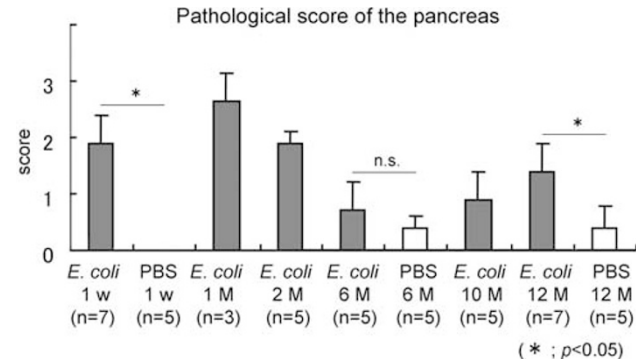


Figure 3 Pathological scores for pancreas tissues. The gray bars indicate the pathological scores of *E. coli*-inoculated mouse pancreas tissue. The white bars indicate the pathological scores of PBS-inoculated mouse pancreas tissue. The error bar indicates + s.d. (*P<0.05, n.s., not significant).

in the salivary glands of PBS-inoculated mice, cellular infiltration was none to mild (Figure 4c, d). The cellular infiltrates around the bile ducts were much milder than that in the salivary glands (data not shown). Inflammatory cellular infiltrates in the renal tubules were not induced by repeated *E. coli* inoculations in these mice (data not shown). The inflammatory involvement of the salivary glands appeared to resemble the sclerosing sialadenitis that is occasionally associated with human AIP.¹⁹ These results indicate that an extrapancreatic lesion similar to that occurring in human AIP was induced in the *E. coli*-inoculated mice.

Upregulation of Acquired Immunity in *E. Coli*-Inoculated C57BL/6 Mice

To clarify the cell subsets infiltrating the pancreas, we next performed immunohistochemical staining. In the *E. coli*-inoculated mice, CD3-positive cells were predominantly observed in lymphocytic populations in the exocrine pancreas at 1, 2, 6, and 12 months after the final *E. coli* inoculation (Figure 5a, d, g, j). On the other hand, fewer B220-positive B cells (Figure 5b, e, h, k) and F4/80-positive monocytes/macrophages were observed in these mice (Figure 5c, f, i, l).

The serum IgG level is known to be elevated in patients with AIP;²⁰ however, IgG4 does not exist in mice. Therefore, we studied the total IgG levels in sera samples obtained 12 months after the final *E. coli* or PBS inoculation. The amount of IgG was about four times higher in the *E. coli*-inoculated mouse sera than in the PBS-inoculated mouse sera, and this difference was statistically significant (Figure 6a, b). Taken together, these results suggest the upregulation of acquired immunity in *E. coli*-inoculated mice, similar to the situation in patients with AIP.

Autoantibodies in *E. Coli*-Inoculated C57BL/6 Mice Sera

Anti-CA-II and anti-LF are the most frequently detected autoantibodies in human AIP.^{4–6} To determine whether

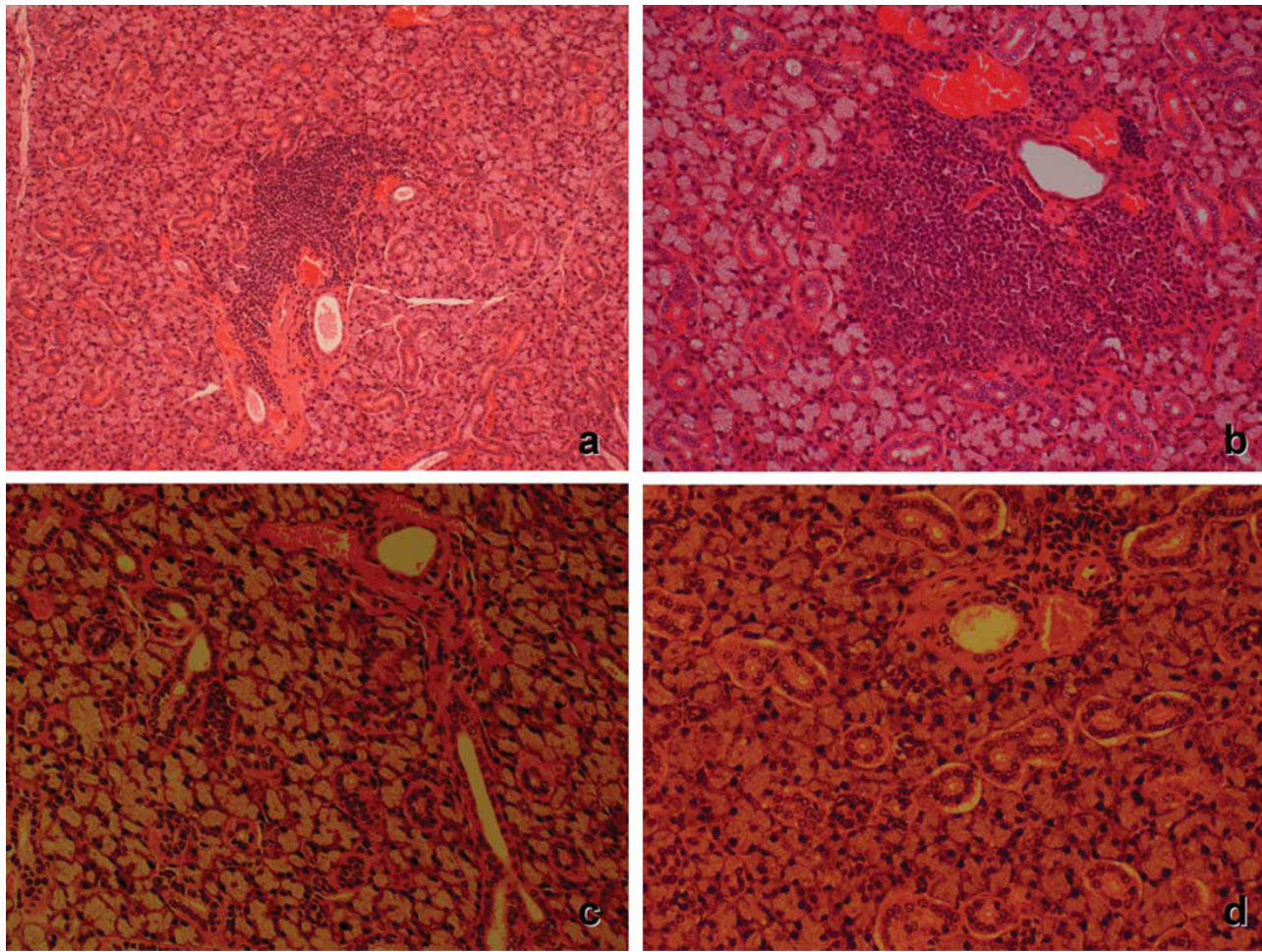


Figure 4 Representative pathological findings of the salivary glands in *E. coli*-inoculated C57BL/6 mice at 6 months (**a**) and 12 months (**b**) after the final *E. coli* inoculation, and at (**c**) 6 months and (**d**) 12 months after the final PBS inoculation (H&E staining).

autoantibodies are generated in repeated *E. coli*-inoculated C57BL/6 mice *in vivo*, anti-CA-II and anti-LF antibodies were measured. The anti-CA-II antibody levels in sera from C57BL/6 mice inoculated with *E. coli* were significantly higher than those in mice inoculated with PBS. The titers of anti-CA-II increased according to time after the final *E. coli* inoculation (Figure 7a, b). In the same set of sera, the anti-LF level was also significantly higher in the *E. coli*-inoculated mice than in the PBS-inoculated mice. The anti-LF also increased over time after the final *E. coli* inoculation (Figure 7c). ANA is also detected in patients with AIP. To detect ANA, the HEp-2 cells were stained with mouse sera. As shown in Figure 6d, ANA developed in C57BL/6 mice after the completion of eight inoculations of heat-killed *E. coli*. Anti-CA-II and anti-LF titers were increased over time, which may reflect that pathological alteration in the inflammatory cellular infiltrates in the pancreas from granulocytes dominance to lymphocytes and plasma cells dominance. Thus, representative autoantibodies produced in human AIP were also detected in *E. coli*-inoculated mice.

Spleen Cell Transfer to RAG2^{-/-} Mice

To examine whether *E. coli*-inoculated C57BL/6 mice spleen cells possess the ability to induce the same alteration in the pancreases of naïve mice, *E. coli*-inoculated C57BL/6 mice spleen cells were i.v. transferred into RAG2^{-/-} mice. At 1 week after the i.v. transfer of the *E. coli*-inoculated C57BL/6 mice spleen cells, the pancreases in the recipient RAG2^{-/-} mice showed cellular infiltration in the exocrine pancreas, especially around the pancreatic ducts (Figure 8a). In representative sections stained immunohistochemically, most of the cellular infiltrates in the exocrine pancreas were CD3 positive (Figure 8b), indicating that these cells originated from the donor *E. coli*-inoculated C57BL/6 mice, because RAG2^{-/-} mice in which the RAG2 gene has been eliminated by gene ‘knockout’ have no mature T or B cells, as a result of the abrogation of V(D)J recombination.²¹ On the other hand, in the pancreases of the recipient RAG2^{-/-} control mice, which were treated i.v. with spleen cells obtained from C57BL/6 mice inoculated weekly with PBS for 8 weeks, cellular infiltration was scored as none to quite mild (Figure 8c).

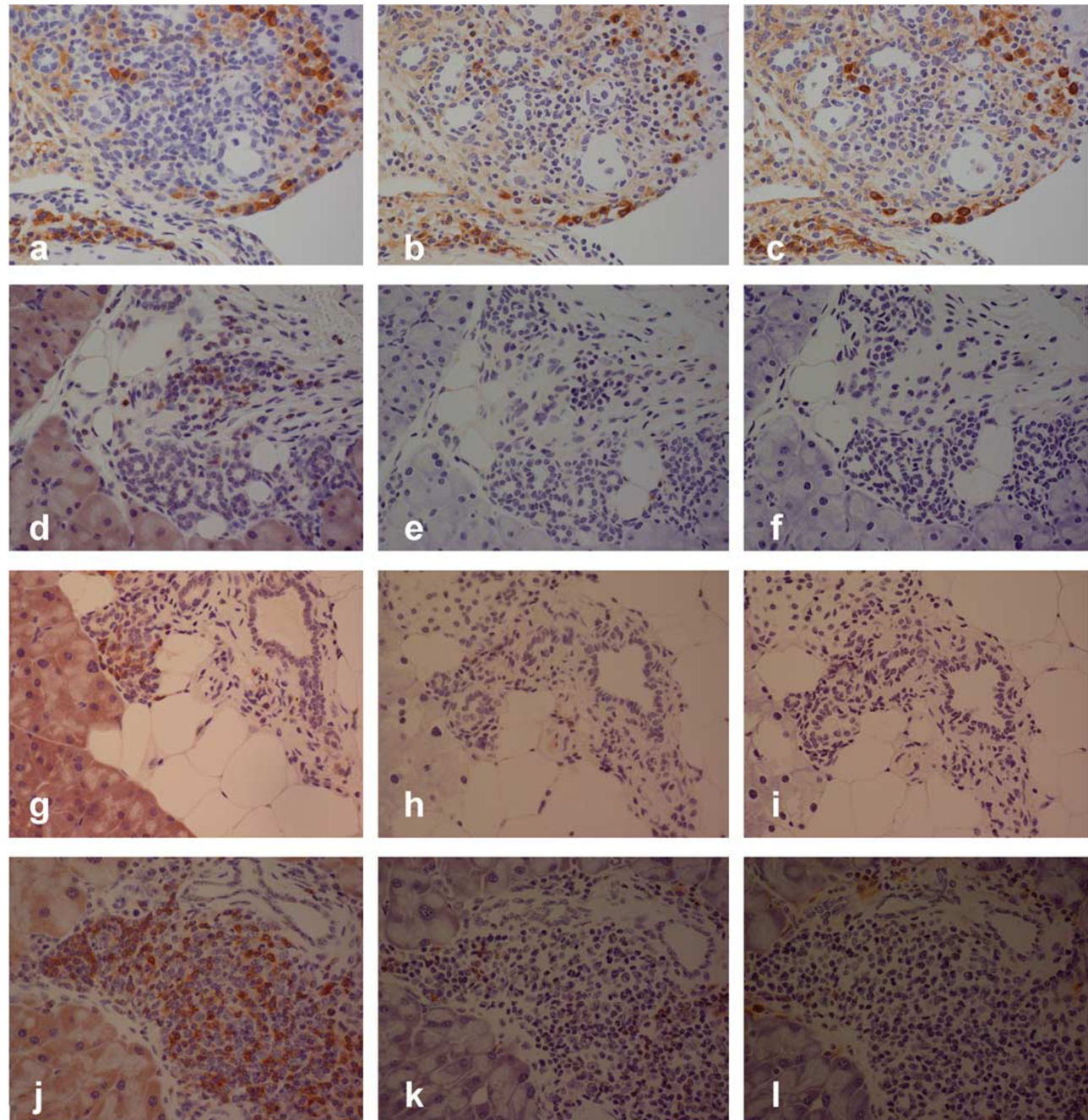


Figure 5 Immunostaining of various molecules in *E. coli*-inoculated C57BL/6 mouse pancreas at 1 month (**a–c**), 2 months (**d–f**), 6 months (**g–i**) and 12 months after the final *E. coli* inoculation. Immunoreactivities to CD3 (**a, d, g, j**), B220 (**b, e, h, k**), and F4/80 (**c, f, i, l**) antigens in the pancreas are shown.

and donor-originated CD3-positive cells were not detected (Figure 8d). These results indicate that autoimmune mechanisms are likely involved in the pathogenesis of *E. coli*-triggered pancreatitis in C57BL/6 mice.

DISCUSSION

We previously reported that chronic exposure to a Gram-positive bacteria, *S. i*, resulted in PBC-like nonsuppurative destructive cholangitis in the liver of BALB/c mice. However,

in our observations, repeated i.p. inoculations with avirulent *E. coli* resulted in none to mild inflammation around the bile duct in the liver.¹⁸ Strikingly, in this study, the repeated exposure of C57BL/6 mice to heat-killed *E. coli* resulted in AIP-like pathological alterations in the pancreas beginning 1 week after the completion of an 8-week *E. coli* exposure period. In the same mice, pathological alterations were detected in the salivary glands, but not around the bile ducts in the liver. Furthermore, AIP-like pathological alterations in

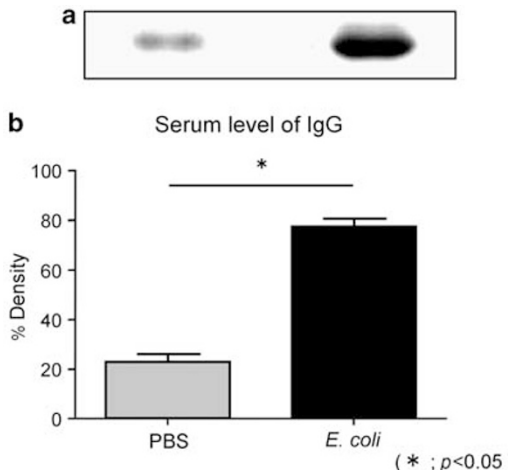


Figure 6 Serum levels of IgG in sera samples obtained up to 12 months after the final inoculation of *E. coli* or PBS. (a) Mouse IgG in 5 μ l of each serum sample was immunoprecipitated using protein G Sepharose. The bound IgG was run on a 12% acrylamide gel and stained with Coomassie brilliant blue R-250. (b) The intensity of each band on the gel was measured using the ImageJ program/gel analyzer option. $*P < 0.05$.

the pancreas were also observed in repeated heat-killed *E. coli*-inoculated BALB/c mice (unpublished data). In AIP patients, a close relationship between HLA DRB1*0405 and DRB1*0401 has been reported.^{7,9} However, no significant difference between the responsiveness to repeated heat-killed *E. coli* inoculation was noted between C57BL/6 and BALB/c mice in this experimental protocol. To clarify whether MHC class II antigens have some role(s) in our *E. coli*-triggered AIP-like pancreatitis-harboring mouse model, further examinations, such as changing the doses of bacteria loading and the duration of bacteria exposure, using numerous mouse strains are needed.

Recently, AIP has been classified into two types: type 1, comprised of LPSP, and type 2, comprised of IDCP or GEL-positive pancreatitis.⁵ GEL is characterized by the massive infiltration of granulocytes into the pancreatic parenchyma and ductal epithelium.^{5,6} In our repeated *E. coli*-inoculated mice, the marked cellular infiltration consisted mainly of granulocytes, and the granulocytic infiltration was particularly centered in the ductal systems, with intracaliber abscesses with or without the destruction of epithelial cells and fibrosis commonly seen (Figure 1); these observations closely resembled the characteristics of GEL in human AIP.²²

The GEL-like inflammation in the pancreas persisted for 1–2 months after the final *E. coli* inoculation in mice without additional *E. coli* inoculations, that is, during a bacterial exposure-free period (Figure 2). However, the predominance of cellular infiltrates were shifting from granulocytes to lymphocytes and plasma cells. The inflammation in the exocrine pancreas then appeared to regress and was replaced with fatty tissues ~6 months after the final *E. coli* inoculation (Figure 2). The meaning of the replacement of the acinar

cells with the fatty tissue is unclear. Clarifying the mechanisms and role(s) of the replacement with fatty tissue in these AIP-like pancreatitis-harboring mice would be of interest. We further investigated the pancreas in long-term additional *E. coli* inoculation-free mice. At 10–12 months after the final *E. coli* inoculation, infiltrations of lymphocytes, plasma cells, and granulocytes into the pancreas and duct-centric fibrosis were observed in the exocrine pancreas, perhaps, the histology of which might be closer to LPSP (Figure 2). In addition, inflammation in the salivary glands was also observed (Figure 3).

Oldstone reported that molecular mimicry has been proposed as a pathogenetic mechanism for autoimmune disease. This hypothesis was based, in part, on evidence of an association between infectious agents and autoimmune disease and the observation of cross-reactivity between immune reagents or host 'self' antigens and microbial determinants.²³ The most probable mechanism is the generation of cytotoxic cross-reactive effector lymphocytes or antibodies that recognize specific determinants on target cells. For the induction of cross-reactivity, immune-mediated injury could be induced even after the immunogen has been removed.²³ A similar mechanism might be upregulated in the *E. coli*-inoculated AIP-like pancreatitis-harboring mice reported in this study. Determining the bacterial component(s) and/or molecular mimicry that are the target of the autoimmune response in this mouse model might help us to clarify the pathogenesis of AIP.

A histopathological analysis of aly/aly mice, a spontaneous model for Sjögren's syndrome, revealed the systemic inflammation of exocrine glands including the lacrimal and salivary glands, as well as the pancreas. Interestingly, the pancreatic islets were completely exempted from the damage.²⁴ In our repeated *E. coli*-inoculated mice, inflammation in the islets was also very minimal to absent, compared with in the exocrine cells. Thus, the endocrine islets might be more resistant to the destructive effects of the cell infiltrates or they might not possess the target antigens.

IgG4-secreting plasma cells and T-cell-dominant infiltration are characteristic features of AIP.²⁰ As IgG4 does not exist in mice, we were not able to assess the upregulation of IgG4 in this mice model. In *E. coli*-inoculated mice, CD3-positive cells were predominant throughout the sequential pathological observation, compared with B220-positive B cells and F4/80-positive macrophage/monocytes (Figure 4), and an increasing level of serum IgG was observed (Figure 5). These results also indicated that our mouse model is similar to AIP.²⁵ In AIP, titers of anti-CA-II, anti-LF ANA, and rheumatoid factor are variably increased. From 1 week after the final *E. coli* inoculation, anti-LF and anti-CA-II antibodies, as well as ANA, were generated in the sera of *E. coli*-inoculated mice (Figure 6). The antibody titers increased as the granulocyte predominance shifted to a predominance of lymphocytes and plasma cells. Novel antibody-associated AIP was reported.²⁶ To study titers of plasminogen-binding

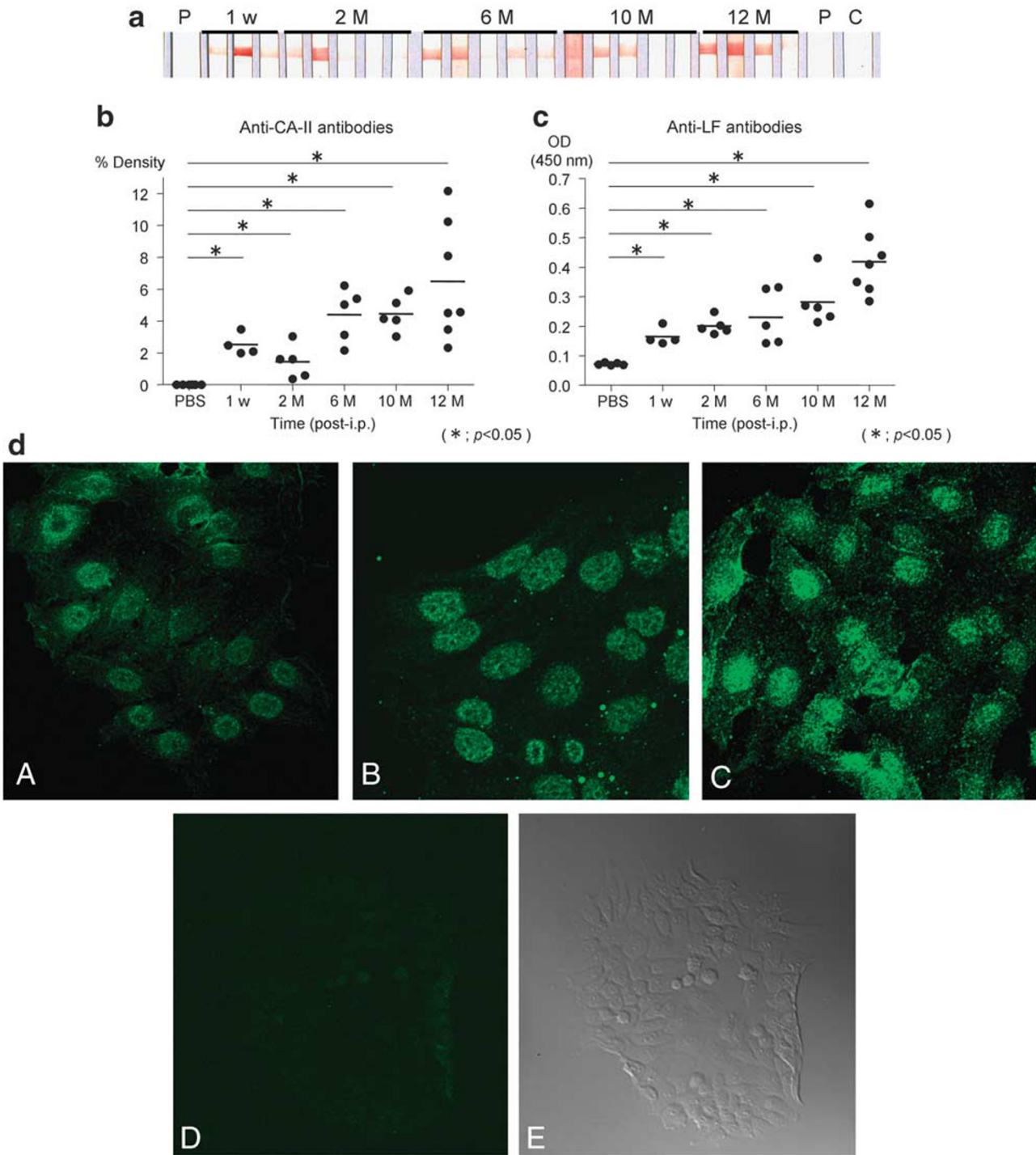


Figure 7 Detection of anti-CA-II and anti-LF in the sera of *E. coli*-inoculated mice. **(a)** Six groups of mice were compared according to the time after the final *E. coli* inoculation. Nitrocellulose membrane transferred with CA-II (50 µg per 75 × 92 mm²) was cut into strips (5-mm widths). The wells and strips were incubated with each serum sample (1:100 dilution). The bound antibody was detected using peroxidase-conjugated goat anti-mouse IgG, and the percent density of each band on the gel was determined. **(b)** Each symbol represents the mean of triplicate determinations of CA-II. **(c)** Microtiter plates, coated with 10 µg/ml of LF in 100 µl of 50-mM sodium carbonate buffer, were used to detect the serum anti-LF antibodies. Each well was incubated with each mouse serum sample (1:100 dilution), and then incubated with HRP-conjugated anti-mouse IgG. The reaction was read at OD 450 nm. *P<0.05. **(d)** Detection of ANA using HEp-2 cells in sera obtained 1 month (A), 2 months (B), and 12 months (C) after the final *E. coli* inoculation and at 12 months after the final PBS inoculation (D). DIC image of D (E).

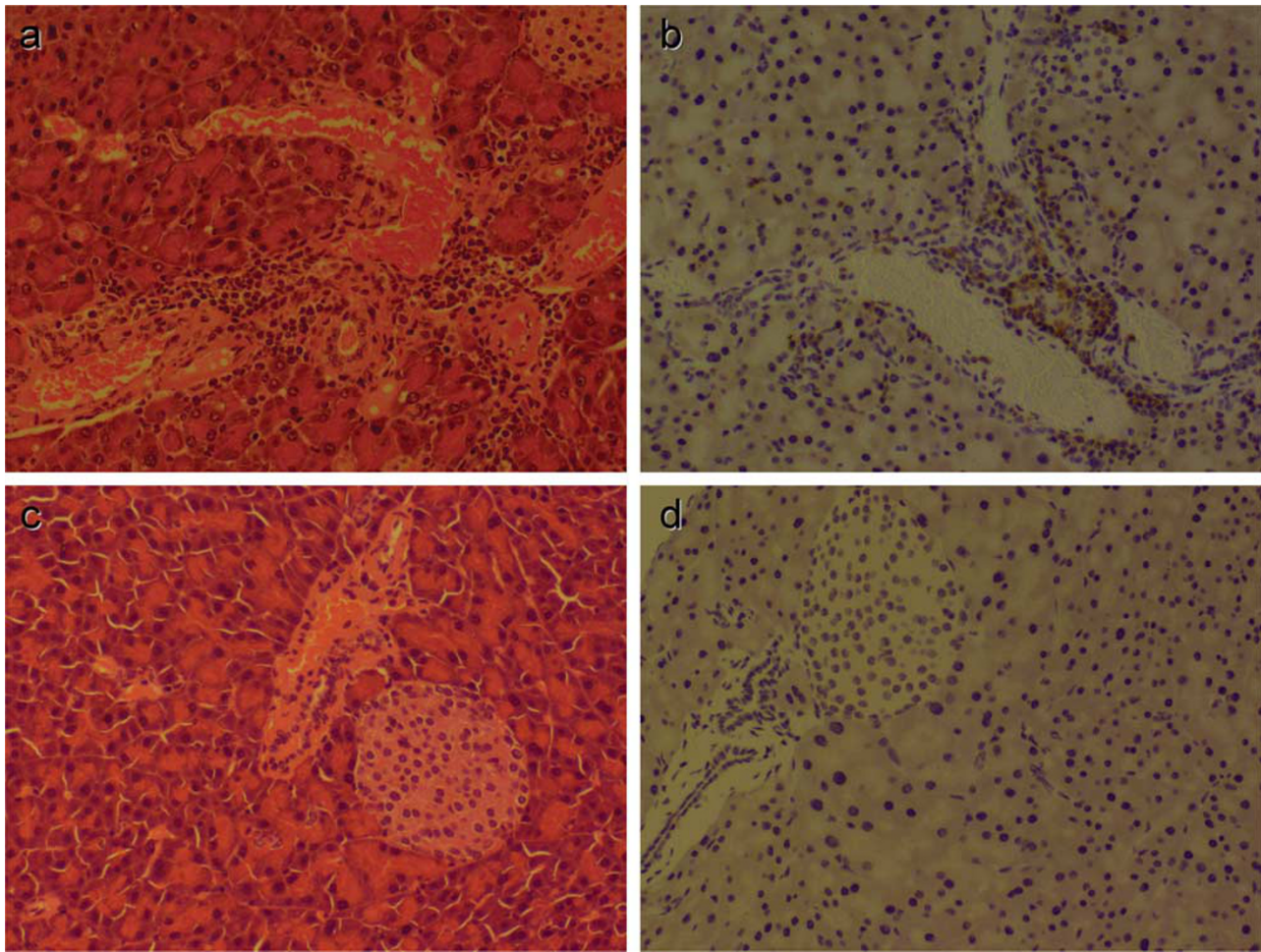


Figure 8 Representative pathological findings of spleen cell-transferred $RAG2^{-/-}$ pancreas tissues. The representative pancreas tissues were obtained at 1 week after the adaptive transfer of spleen cells obtained from *E. coli*-inoculated (**a, b**) and PBS-inoculated mice (**c, d**) (**a, c**: H&E staining; **b, d**: immunoreactivities to CD3).

protein would be worthwhile. These findings suggest that in *E. coli*-inoculated AIP-like pancreatitis-harboring mice, GEL-like inflammation in the pancreas was occurred in early stage, and subsequently, even without additional bacterial stimulation, LPSP-like inflammation might be progressing. In human AIP, there was no report that described about the conversion from IDCP or GEL to LPSP. However, our mice model might suggest one possible pathological rout of disease progression from IDCP or GEL to LPSP. From the aspect of these phenomena, our findings might be of some interest. Furthermore, recently, the number of regulatory T cells has been reported to increase in AIP patients and in a manner that is correlated with the serum IgG4 level, whereas the number of naïve regulatory T cells decreases.²⁷ Further research on the T-cell subsets in this model, including Treg cells, is needed to elucidate the mechanism underlying the elevation in serum IgG in the present mouse model. It would be interesting to investigate the responsiveness of this mouse model to steroid therapy, as the fibroinflammatory process of AIP responds to steroid treatment.^{28–31}

To date, several animal models of AIP have been reported.^{31–35} In most models, the AIP-like disease is induced by the adoptive transfer of autoreactive cells and self-antigens such as CA-II and LF. Similarly, the adaptive transfer of *E. coli*-inoculated mice spleen cells to $RAG2^{-/-}$ mice also reproduced AIP-like pancreatitis in the present study. However, our *E. coli*-inoculated mouse model is quite unique in terms of the development of disease in response to environmental antigens or avirulent bacteria.⁵ From this viewpoint, our model might provide a new insight for clarifying the pathogenesis of AIP. Finally, we have proposed a possible new mechanism of AIP pathogenesis, shown in Figure 9. During the initiation phase, a weak but silently infiltrating pathogen-associated molecular pattern (PAMP)³⁶ and/or antigen(s) such as avirulent bacteria trigger and upregulate the innate immune system. Second, the progressive phase features the persistence of this PAMP attack or stimulation by molecular mimicry, and/or exposure or stimulation from commensal flora possessing the same antigenic epitope that the initial pathogen and/or PAMP

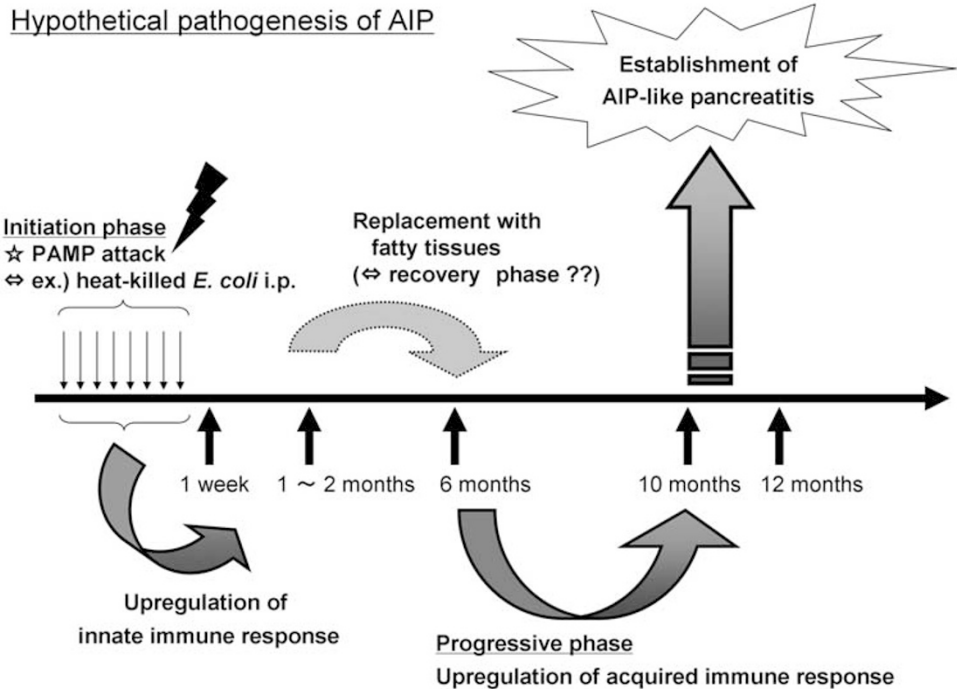


Figure 9 Hypothetical pathogenesis of AIP. In the initiation phase, a silently infiltrating PAMP and/or antigen(s), such as avirulent bacteria, triggers and upregulates the innate immune system. Second, the progressive phase features the persistence of this PAMP attack or stimulation by an unknown self-antigen acting as a molecular mimic and/or exposure or stimulation by commensal flora possessing the same antigenic epitope that the initial pathogen and/or PAMP possessed, upregulating the host immune response to the target antigen. These slowly progressive steps ultimately lead to AIP.

possessed, thereby upregulating the host immune response to the target antigen. These slowly progressive steps eventually lead to the development of AIP. A detailed investigation of the pathological mechanism involved in the presently reported mouse model would provide new hints toward a therapeutic approach for autoimmune epithelial inflammation such as AIP and associated extrapancreatic lesions.

ACKNOWLEDGEMENTS

We thank Ms Noriko Sakayori, Mr Mizuho Karita, Mr Hideyuki Takeiri, Mr Shuichi Iwasaki, and Yasuhide Shigematsu for their skillful technical assistance, and Masamichi Yoshikawa for intensive animal care. This work was financially supported, in part, by grants from the Ministry of Education, Culture, Sports, Science, and Technology of Japan.

DISCLOSURE/CONFLICT OF INTEREST

The authors declare no conflicts of financial interest.

- Sarles H, Sarles JC, Muratore R, et al. Chronic inflammatory sclerosis of the pancreas—an autonomous pancreatic disease? *Am J Dig Dis* 1961;6:688–698.
- Toki F, Kozu T, Oi I, et al. An unusual type of chronic pancreatitis showing diffuse irregular narrowing of the entire main pancreatic duct on ERC—a report of four cases. *Endoscopy* 1992;24:640.
- Yoshida K, Toki F, Takeuchi T, et al. Chronic pancreatitis caused by autoimmune abnormality. Proposal of concept of autoimmune pancreatitis. *Dig Dis Sci* 1995;54:1561–1568.
- Okazaki K, Uchida K, Fukui T. Recent advances in autoimmune pancreatitis: concept, diagnosis, and pathogenesis. *J Gastroenterol* 2008; 43:409–418.
- Park DH, Kim M-H, Chari ST. Recent advances in autoimmune pancreatitis. *Gut* 2009;58:1680–1689.
- Shimosegawa T, Kanno A. Autoimmune pancreatitis in Japan: overview and perspective. *J Gastroenterol* 2009;44:503–517.
- Kawa S, Ota M, Yoshizawa K, et al. HLA DRB1*0405-DQB1*0401 haplotype is associated with autoimmune pancreatitis in Japanese population. *Gastroenterology* 2002;122:1264–1269.
- Murakami T, Hamano H, Ochi Y, et al. Autoimmune pancreatitis and complement activation system. *Pancreas* 2006;32:16–21.
- Ota KM, Katsuyama Y, Hamano H, et al. Two critical genes (HLA-DRB1 and ABCF1) in the HLA region are associated with the susceptibility to autoimmune pancreatitis. *Immunogenetics* 2007;59:45–52.
- Uchida K, Okazaki K, Nishi T, et al. Experimental immune-mediated pancreatitis in neonatally thymectomized mice immune with carbonic anhydrase II and lactoferrin. *Lab Invest* 2002;82:411–424.
- Murphy K, Travers P, Walport M, (eds) *Immunobiology*. Garland Science: New York and London, 2008, pp 62.
- Laine VJO, Nyman KM, Peuravuori HJ, et al. Lipopolysaccharide induced apoptosis of rat pancreatic acinar cells. *Gut* 1996;38: 747–752.
- Vonlaufen A, Xu Z, Daniel B, et al. Bacterial endotoxin: a trigger factor for alcoholic pancreatitis? Evidence from a novel, physiologically relevant animal model. *Gastroenterology* 2007;133:1293–1303.
- Shinkai Y, Rathbun G, Lam KP, et al. RAG-2-deficient mice lack mature lymphocytes owing to inability to initiate V(D)J rearrangement. *Cell* 1992;68:855–867.
- Williams JA, Hathcock KS, Klug D, et al. Regulated costimulation in the thymus is critical for T cell development: dysregulated CD28 costimulation can bypass the pre-TCR checkpoint. *J Immunol* 2005;175:4199–4207.
- Rasband WS. ImageJ 1997–2009. US National Institutes of Health: Bethesda, MD, USA; <http://rsb.info.nih.gov/ij/>.
- Tsiakalou V, Tsangaridou E, Polioudaki H, et al. Optimized detection of circulating anti-nuclear envelope autoantibodies by immunofluorescence. *BMC Immunol* 2006;7:20.

18. Haruta I, Kikuchi K, Hashimoto E, et al. Long-term bacterial exposure can trigger nonsuppurative destructive cholangitis associated with multifocal epithelial inflammation. *Lab Invest* 2010;90: 577–588.
19. Kamisawa T, Funata N, Hayashi Y, et al. Close relationship between autoimmune pancreatitis and multifocal fibrosclerosis. *Gut* 2003; 52:683–687.
20. Hamano H, Kawa S, Horiuchi A, et al. High serum IgG4 concentrations in patients with sclerosing pancreatitis. *N Engl J Med* 2001;344: 732–738.
21. Max EE. Immunoglobulins: molecular genetics. In: Paul WE (ed). *Fundamental Immunology*. Lippincott Williams and Wilkins: Philadelphia, USA, 2008, pp 203–204.
22. Zamboni G, Lüttges J, Capelli P, et al. Histopathological features of diagnostic and clinical relevance in autoimmune pancreatitis: a study on 53 resection specimens and 9 biopsy specimens. *Virchows Arch* 2004;445:552–563.
23. Oldstone MBA. Molecular mimicry and immune-mediated diseases. *FASEB J* 1998;12:1255–1265.
24. Tsubata R, Tsubata T, Hiai H, et al. Autoimmune disease of exocrine organs in immunodeficient alymphoplasia mice: a spontaneous model for Sjögren's syndrome. *Eur J Immunol* 1996;26: 2742–2748.
25. Okazaki K, Chiba T. Autoimmune pancreatitis. *Gut* 2002;51:1–4.
26. Fulloni L, Lunardi C, Simone R, et al. Identification of a novel antibody associated with autoimmune pancreatitis. *N Engl J Med* 2009;361: 2135–2142.
27. Miyoshi H, Uchida K, Taniguchi T, et al. Pancreas Circulating Naïve and CD4+CD25high regulatory T cells in patients with autoimmune pancreatitis. *Pancreas* 2008;36:133–140.
28. Kamisawa T, Shimosegawa T, Okazaki K, et al. Standard steroid treatment for autoimmune pancreatitis. *Gut* 2009;58:1504–1507.
29. Ryu JK, Chung JB, Park SW, et al. Review of 67 patients with autoimmune pancreatitis in Korea. *Pancreas* 2008;37:377–385.
30. Frulloni L, Scattolini C, Falconi M, et al. Autoimmune pancreatitis: differences between the focal and diffuse forms in 87 patients. *Am J Gastroenterol* 2009;104:2288–2294.
31. Kamisawa T, Okamoto A, Wakabayashi T, et al. Appropriate steroid therapy for autoimmune pancreatitis based on long-term outcome. *Scand J Gastroenterol* 2008;43:609–613.
32. Uchida K, Okazaki K, Nishi T, et al. Experimental immune-mediated pancreatitis in neonatally thymectomized mice immunized with carbonic anhydrase II and lactoferrin. *Lab Invest* 2002;82:411–424.
33. Boomershine CS, Chamberlain A, Kendall P, et al. Autoimmune pancreatitis results from loss of TGF β signalling in S100A4-positive dendritic cells. *Gut* 2009;58:1267–1274.
34. Qu WM, Miyazaki T, Terada M, et al. A novel autoimmune pancreatitis model in MRL mice treated with polyinosinic: polycytidylic acid. *Clin Exp Immunol* 2002;129:27–34.
35. Sakaguchi Y, Inaba M, Tsuda M, et al. The Wistar Bonn Kobori rat, a unique animal model for autoimmune pancreatitis with extrapancreatic exocrinopathy. *Clin Exp Immunol* 2008;152:1–12.
36. Marsland BJ, Kopf M. Toll-like receptors: paving the path to T cell-driven autoimmunity? *Curr Opin Immunol* 2007;19:611–614.